Gain Evolution in the HRC-I

J. Posson-Brown (CXC/SAO)
R. H. Donnelly (CXC/SAO)

27 October 2003

Abstract

Since launch, calibration observations of several sources, including AR Lac, Cas A, G21.5-0.9, and HZ 43, have been taken with the HRC-I to monitor the detector's performance. Analysis of these observations, examining the median source pulse height amplitude (PHA) as a function of time, reveals gain fatigue in the HRC-I. We find that since the voltage adjustment in October 1999, the gain at the nominal aimpoint of the detector has declined by roughly 19%. At the twenty offset positions monitored with AR Lac, we find declines in gain ranging from roughly 4 to 9%, decreasing with radial distance from the aimpoint. This gradual lowering of the gain has not yet affected the quantum efficiency (QE). However, if left unchecked, the gain fatigue will eventually cause events to drop below the lower level discriminator (LLD), leading to a decline in QE.

Analysis

We began our analysis with AR Lac, a point source that is regularly observed to monitor the HRC-I gain at the aimpoint and twenty offset positions (see Table 1). After this analysis revealed gain fatigue in the detector, we examined observations of other standard calibration sources (HZ 43, Cas A, and G21.5-0.9) taken at the aimpoint. These observations are identified in Tables 2-4.

For each source, we analyzed the Level 1 event lists filtered on the nominal good time intervals (GTIs) provided in the standard filter files. The Level 1 event lists were selected to avoid changes in the data due to revisions of the standard pipeline processing over the years.

We extracted PHAs of events within a circular region around each source. We then calculated the median source PHA for each observation after rejecting events from the highest channel (255). This channel is often contaminated by a second peak, consisting of source events that are not well-understood, and would probably be excluded by a typical user. Channel 255 events are under investigation, but in the meantime we note that rejecting these events affects the median PHA by at most a few channels, and thus does not impact our results in any significant way.

For observations of AR Lac and HZ 43 at the aimpoint, we estimated the average rates of change with time of the median PHA and the width of the distribution (as measured by the standard deviation of the median) by doing linear least-squares fits to the data. Finally, we fit Gaussians to the PHA distributions for observations of AR Lac and HZ 43 taken at the aimpoint to show qualitatively how the distributions are evolving. Note that the parameters from the Gaussian fits were not used in our quantitative analysis to estimate the rate of gain decline.

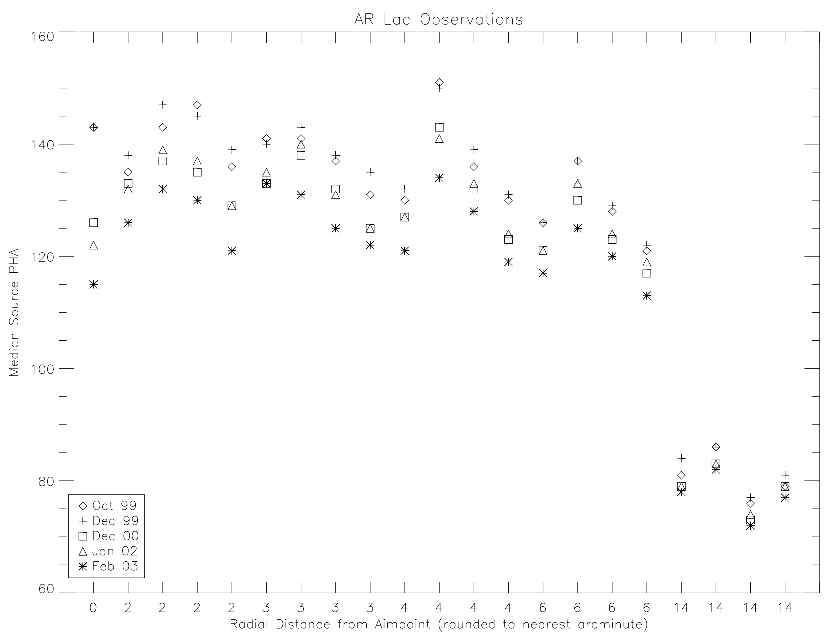

Figure 1: Median PHA vs Radial Distance

Y Offset	Z Offset	Radial Dist	Oct 99	Dec 99	Dec 00	Jan 02	Feb 03
arcmin	arcmin	arcmin	ObsID	ObsID	ObsID	ObsID	ObsID
0	0	0	1321	1484	0996	2608	4294
2	0	2	1324	1485	2345	2617	4303
0	2	2	1342	1491	2351	2611	4297
-2	0	2	1336	1489	2349	2610	4296
0	-2	2	1330	1487	2347	2618	4304
2	2	2.83	1345	1492	2352	2604	4290
-2	2	2.83	1339	1490	2350	2619	4305
-2	-2	2.83	1333	1488	2348	2624	4310
2	-2	2.83	1327	1486	2346	2609	4295
4	0	4	1348	1493	2353	2620	4306
0	4	4	1366	1499	2359	2606	4293
-4	0	4	1360	1497	2357	2621	4307
0	-4	4	1354	1495	2355	2612	4300
6	0	6	1351	1494	2354	2605	4291
0	6	6	1369	1500	2360	2607	4292
-6	0	6	1363	1498	2358	2613	4299
0	-6	6	1357	1496	2356	2614	4298
10	10	14.14	1372	1501	2361	2615	4301
-10	10	14.14	1381	1504	2364	2616	4302
-10	-10	14.14	1378	1503	2363	2623	4309
10	-10	14.14	1375	1502	2362	2622	4308

Table 1: AR Lac Observations

Results

For all 21 monitored positions on the detector with AR Lac, we find that the median PHA has dropped from October 1999 to February 2003. This drop is most dramatic at the aimpoint (not surprising since this area receives the most photons) at about 19%. For the twenty offset positions monitored, the drop ranges from roughly 4 to 9%, decreasing with radial distance from the aimpoint. This is summarized in Figure 1. The data are ordered along the x-axis by radial distance from the aimpoint. Within each set at a given distance, they are arranged in counter-clockwise order by their position in the y-z plane of the detector, starting at the positive y-axis.

The changes in the AR Lac PHA profiles at the aimpoint are shown qualitatively by the Gaussian fits in Figure 2. The Gaussians have been normalized by the total counts in each extracting area to facilitate easy comparison. Note that not only is the median declining with time, but the distributions are becoming narrower.

To explore if the gain loss is energy dependent, we compared the median source PHAs for six observations of HZ 43 taken at the nominal aimpoint over the past few years. We detect emission from HZ 43 primarily in the range of 0.06 to 0.20 keV, while emission from AR Lac peaks around 1 keV. We find that the median PHA for HZ 43 has dropped by approximately 16% and that the PHA distributions are becoming narrower, similar to the trends seen with AR Lac. Figure 3 shows Gaussian fits to the HZ 43 PHA profiles, normalized by total counts.

Figure 4 shows the median source PHAs from the HZ 43 and AR Lac observations at the aimpoint as a function of time. The solid lines are projections of the earliest value in each data set. Thus, deviations from these horizontal lines indicate gain evolution. The gain loss as witnessed by HZ 43 is linear with time (dot-dash lin e), whereas the AR Lac medians are not well-fit by a line. Two linear least-squares fits to the AR Lac data are shown. The dashed line excludes the first two points, and within errors has the same slope as the HZ 43 fit, while the dotted line includes all points and gives a steeper rate of decline. We use this steeper slope - the "worst-case scenario" - to approximate when the gain fatigue will have a non-trivial impact on the detector's quantum efficiency. (We define a "non-trivial impact" as 5% of source events falling below the Lower Level Discriminator value of 8.) We estimate that it will be over 6 years until this occurs.

As a final step, we examined the median PHAs of our two extended

ObsID	Obs Date
1514	Feb 00
1000	Jan 01
1001	Jul 01
2600	Jan 02
2602	Jul 02
3714	Jan 03

Table 2: HZ 43 Observations

ObsID	Obs Date
1549	Jan 01
1550	Jul 01
2871	Feb 02
2878	Aug 02
2602	Jul 02
3698	Mar 03

Table 3: Cas A Observations

calibration sources, G21.5-0.9 and Cas A. The gain fatigue is seen by these sources as well. Figure 5 shows the median PHAs over time for all four of the calibration sources. The data for each source are normalized to the intial observation for that source.

ObsID	Obs Date
1406	Oct 99
142	Feb 00
144	Sep 00
1555	Mar 01
1556	Jul 01
2867	Mar 02
2874	Jul 02
3694	May 03

Table 4: G21.5-0.9 Observations

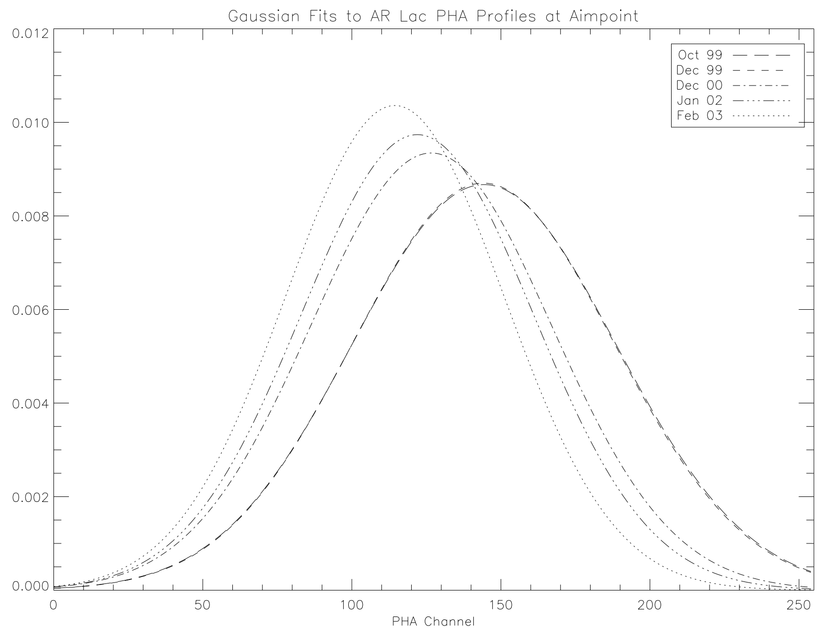

Figure 2: Evolution of AR Lac PHA profiles

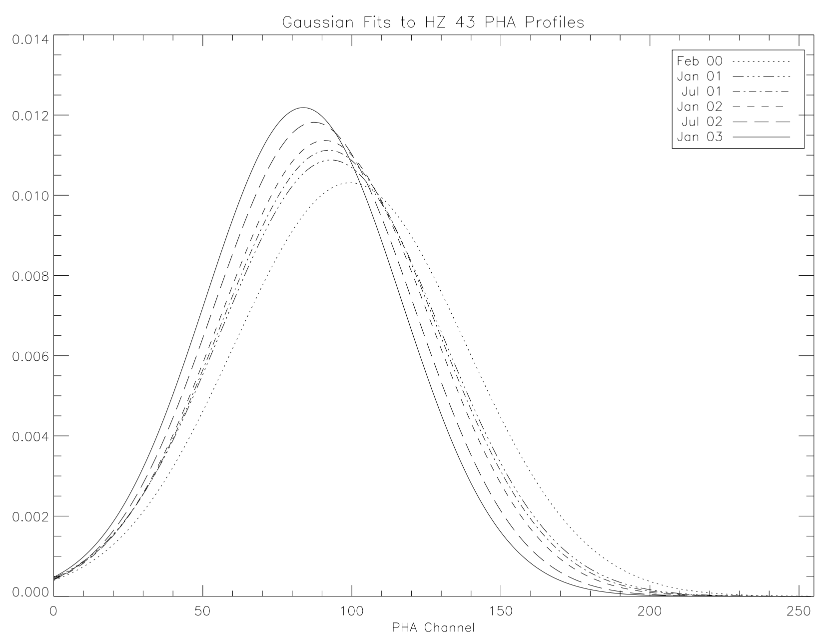

Figure 3: Evolution of HZ 43 PHA profiles

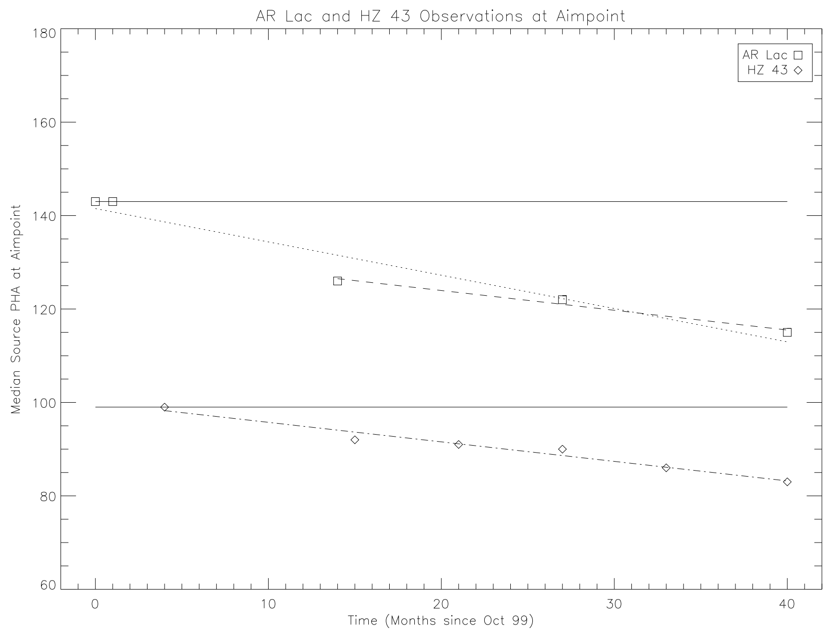

Figure 4: Median PHA vs time

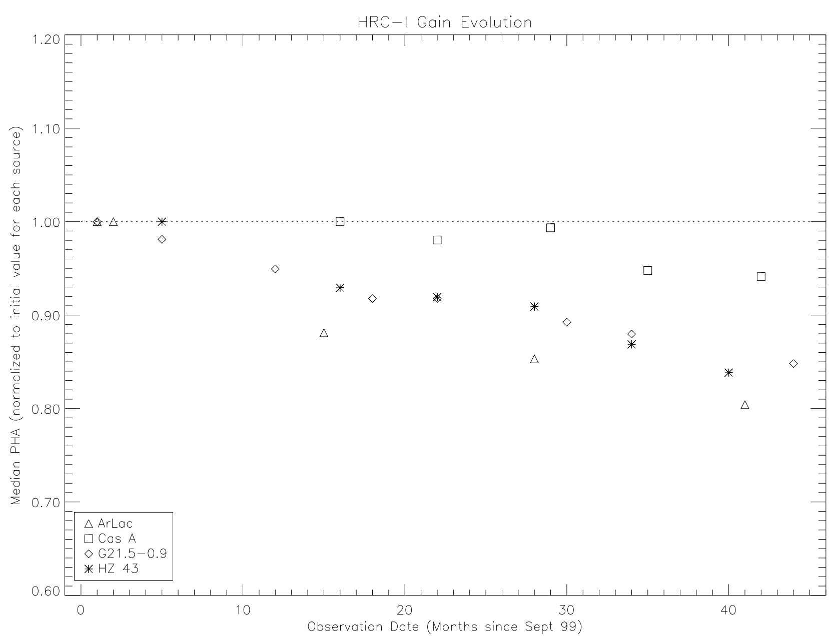

Figure 5: Evolution of median PHA for all four sources